Catalysis Today 213 (2013) 127–134

Contents lists available at SciVerse ScienceDirect

Catalysis Today

journal homepage: www.elsevier.com/locate/cattod

Effect of gadolinium on the catalytic properties of iron oxides for WGSR

Caio Luis Santos Silva[a], Sérgio Gustavo Marchetti[b], Arnaldo da Costa Faro Júnior[c], Tatiana de Freitas Silva[d], José Mansur Assaf[d], Maria do Carmo Rangel[a,*]

[a] GECCAT Grupo de Estudos em Cinética e Catálise, Instituto de Química, Universidade Federal da Bahia, Campus Universitário de Ondina, Federação, 40 170-280 Salvador, Bahia, Brazil
[b] CINDECA, Facultad de Ciencias Exactas, Universidad Nacional de La Plata, calle 47 y 115, 1900 La Plata, Argentina
[c] Universidade Federal do Rio de Janeiro, Ilha do Fundão, 21941-909 Rio de Janeiro, Rio de Janeiro, Brazil
[d] Universidade Federal de São Carlos, Rod. Washington Luiz, Km 235, 13565-905 São Carlos, São Paulo, Brazil

ARTICLE INFO

Article history:
Received 19 December 2012
Received in revised form 18 February 2013
Accepted 20 February 2013
Available online 11 May 2013

Keywords:
Hydrogen
WGSR
Gadolinium ferrite
Hematite
Magnetite
Iron carbide

ABSTRACT

Due to the need for energy supply through cleaner and more efficient technologies, the interest for the water gas shift reaction (WGSR) has increased especially due to its role in purifying hydrogen-rich streams. In order to find alternative catalysts for this reaction, the effect of gadolinium and its amount on the properties of iron oxide-based catalysts was studied in this work. Samples with different gadolinium to iron molar ratio (0.05; 0.1 and 0.15) were prepared by sol–gel method and characterized by chemical analysis, thermogravimetry, differential scanning calorimetry, infrared spectroscopy, X-ray diffraction, Mössbauer spectroscopy, specific surface area measurements and thermoprogrammed reduction. The catalysts were evaluated in WGSR at 1 atm in the range of 250–400 °C. Hematite and gadolinium ferrite were detected for all fresh catalysts based on iron and gadolinium while magnetite and iron carbides and gadolinium oxide were found for the spent ones. The specific surface area increased due to gadolinium, related to its role as spacer. Gadolinium made the reduction of Fe^{3+} and Fe^{2+} species more difficult for all catalysts and then inhibited the production of iron carbides during reaction, increasing the activity. The catalyst with Gd/Fe = 0.10 showed the highest activity that was assigned to its highest specific surface area, which exposed more active sites. No methane or ethane was found indicating that the iron carbides were inactive to Fischer–Tropsch synthesis under reaction conditions.

1. Introduction

Nowadays, hydrogen is primarily produced from hydrocarbons or alcohols through reforming processes. Regardless the kind of reforming (steam reforming, partial oxidation, dry reforming or autothermal reforming), the reactor effluent typically contains mixtures of hydrogen, carbon monoxide, carbon dioxide and steam besides unreacted hydrocarbon [1]. The removal of carbon monoxide from this hydrogen-rich stream is essential for many processes since it can irreversibly poison most of metallic catalysts used in chemical and petrochemical processes [2,3]. Carbon monoxide can also poison platinum electrocatalysts in proton exchange membrane fuel cell (PEMFC), one of the most promising technologies for the production of clean energy [4]. An efficient and widely used way to purify hydrogen-rich streams is provided by water gas shift reaction (WGSR) [2]. This reaction has a considerable technological importance because of its high efficiency in reducing the amount of carbon monoxide generated in the reforming of natural gas or hydrocarbons. In addition, it allows the adjustment of synthesis gas composition, a mixture of carbon monoxide and hydrogen largely used in many industrial processes such as methanol synthesis and Fischer–Tropsch reaction [2,5].

The reaction is reversible and exothermic, favored by low temperatures and large amounts of steam. However, in order to obtain high conversions for economical purposes, the WGSR is usually performed in two stages in industrial processes. The first one occurs in the range of 350–420 °C under favorable kinetic conditions and is known as HTS (high temperature shift) while the other step, called LTS (low temperature shift), is often performed at temperatures around 200–250 °C. For commercial use, iron-based (e.g., Fe/Cr/Cu) and copper-based (e.g., Cu/Zn/Al) catalysts have usually been used for HTS and LTS reactions, respectively [2,5,6]. The HTS catalysts are based on iron oxide promoted with chromium oxide and show several advantages such as low cost, thermal stability and resistance against poisons [2,5,7]. They are commercialized as hematite (α-Fe_2O_3) and are reduced in situ to produce magnetite (Fe_3O_4) which is the active phase. The latest generation of such catalysts also contains copper, which acts as an electronic promoter leading

* Corresponding author. Tel.: +55 7133790922; fax: +55 7132374117.
E-mail addresses: mcarmov@ufba.br, mcarmov@gmail.com (M.d.C. Rangel).

0920-5861/$ – see front matter © 2013 Elsevier B.V. All rights reserved.
http://dx.doi.org/10.1016/j.cattod.2013.02.025

to an increase in the catalytic activity [8,9]. Several studies [2,5,10] have showed that chromium oxide (Cr_2O_3) delays magnetite sintering, avoiding the loss of specific surface area of the catalyst during operation. However, due to the carcinogenic nature of chromium, there is a need to search for alternative dopants for such catalysts. Therefore, several studies have been carried out aiming to replace chromium by other dopants [3,8,11–15] as well as to find alternative catalysts for WGSR [16–21].

With this goal in mind, gadolinium-containing iron oxides were studied in this work, in order to find alternative catalysts for WGSR. The benefic effect of gadolinium regarding the activity of iron compounds was previously demonstrated by Tsagaroyannis et al. [18]. They have found that gadolinium ferrites were promising catalysts for WGSR, being more active than some industrial ones, their activities depending on the preparation method. In the present work, we have investigated the effect of different amounts of gadolinium concerning iron oxide activity (prepared by a different method) in WGSR using a stream composition close to the industrial one.

2. Experimental

2.1. Catalyst preparation

The starting materials used for the preparation of the catalysts were as following: gadolinium (III) nitrate hexahydrate, $Gd(NO_3)_3{\cdot}6H_2O$ (Aldrich, 99.9%), iron (III) nitrate nonahydrate, $Fe(NO_3)_3{\cdot}9H_2O$ (VETEC, ≥98%), and ammonium hydroxide, NH_4OH (Aldrich, ACS Grade). These compounds were used without further purification.

Samples were prepared by precipitation by mixing simultaneously iron nitrate ($Fe(NO_3)_3{\cdot}9H_2O$), gadolinium nitrate ($Gd(NO_3)_3{\cdot}6H_2O$) and ammonium hydroxide solutions at 25 °C. Solids with Gd/Fe molar ratios of 0.05, 0.10 and 0.15 were obtained besides pure iron oxide and gadolinium oxide. For preparing the gadolinium-poorest sample (Gd/Fe = 0.05), 250 mL of a gadolinium nitrate solution (0.05 mol L^{-1}) were added simultaneously with 250 mL of an iron nitrate solution (1.00 mol L^{-1}) and 250 mL of an ammonium hydroxide solution (25%) to a beaker containing water, under stirring. After the complete mixture of the reactants, the pH was adjusted o 11 and the sol was kept under stirring for 30 min. It was then centrifuged (2500 rpm, 5 min), the gel washed with water to remove ammonium and nitrate ions from the solid and then centrifuged again, these steps were repeated five times. The gel was dried in an oven at 120 °C, for 24 h. After drying, the solid (catalyst precursor) was ground and sieved in 100 mesh. The solid was then heated (10 °C min^{-1}) under nitrogen flow (100 mL min^{-1}) at 800 °C, for 2 h. For preparing the samples with different gadolinium contents (Gd/Fe = 0.10 and 0.15) the same experimental procedure was followed but varying the solution concentrations (0.10 and 0.15 mol L^{-1} of gadolinium nitrate, respectively). The same experimental procedure was followed to prepare pure iron oxide and gadolinium oxide to be used as references.

2.2. Catalyst characterization

The catalysts were characterized by chemical analysis, thermogravimetry (TG), differential scanning calorimetry (DSC), Fourier transform infrared spectroscopy (FTIR), X-ray diffraction (XRD), specific surface area measurements, Mössbauer spectroscopy and temperature programmed reduction (TPR).

Iron and gadolinium contents were determined by X-ray fluorescence (XRF) in a Bruker S2PICOFOX spectrometer consisting of a molybdenum anode metal-ceramic X-ray tube (50 kV, 600 μA), a multilayer monochromator, a 30 mm^2 silicon drift detector and an automatic sample changer. The experiments of thermogravimetry (TG) and differential scanning calorimetry (DSC) were performed on the catalyst precursors in a TA Instruments SDT 2670. The sample (0.010 g) was heated at 10 °C min^{-1} in the range of 35–900 °C, under nitrogen flow (30 mL min^{-1}). Fourier transform infrared spectroscopy (FTIR) analyses were performed in a Perkin Elmer model Spectrum One, using samples diluted in potassium bromide discs with a 1:100 ratio. The spectra were recorded in the region between 4000 and 400 cm^{-1}, using 32 scans and a resolution of 4 cm^{-1}.

X-ray diffraction measurements were performed at room temperature in a Shimadzu XRD-6000 model equipment with CuKα radiation (λ = 1.54059 Å) generated at 40 kV and 30 mA with a nickel filter. The diffractograms were obtained with a scanning velocity of 2° min^{-1} in the range of 10–80° (2θ). The specific surface areas were measured by nitrogen adsorption at −196 °C using a Micromeritics ASAP 2010 instrument and calculated using the BET model. Before analysis, the sample (0.5 g) was heated up to 200 °C under vacuum in order to remove volatiles from the solids.

Mössbauer spectra were obtained in a spectrometer with 512 channels with constant acceleration and geometry of transmission. A source of ^{57}Co in Rh matrix of nominally 50 mCi was used. Velocity calibration was performed against a 12 μm-thick α-Fe foil. All isomer shifts (δ) mentioned in this paper are referred to this standard. For each component of the spectra, Lorentzians lines of the same width were used. The spectra were obtained at room temperature and folded to minimize geometric effects, being evaluated using a commercial computer fitting program named Recoil. The temperature-programmed reduction analyses were carried in a Zeton Altamar AMI 90 apparatus equipped with a TCD detector. Before analyses, the samples (0.3 g) were heated up to 400 °C under argon flow (30 mL min^{-1}), in order to remove water and then cooled to 35 °C. During analyses, the samples were heated from 35 to 1000 °C under a flow (30 mL min^{-1}) of a 10% H_2/Ar mixture.

2.3. Catalyst evaluation

The catalysts were evaluated in WGSR at atmospheric pressure in the range of 250–400 °C in a tubular fixed bed microreactor using stream (135 mL min^{-1}) with steam to process gas molar ratio (3.7% CO, 3.7% CO_2, 22.2% H_2, 70.4% N_2) of 0.6 (steam/carbon monoxide molar ratio 16:1) and 150 mg of catalyst. The gaseous effluent was analyzed by on line gas chromatography, using a Varian Model 3800 instrument equipped with 2 TCD detectors. Other runs were carried out at 400 °C, for 6 h over all catalysts. After reaction, the catalysts were characterized by X-ray diffraction, Mössbauer spectroscopy and specific surface area measurements in order to follow the changes which might have occurred during reaction.

3. Results and discussion

Table 1 shows the results of the chemical analysis for the catalysts. For all samples the experimental Gd/Fe molar ratios were the same as the expected values, indicating that the experimental

Table 1
Chemical composition of the catalysts. G: gadolinium oxide; F: iron oxide; FG05, FG10 and FG15: gadolinium and iron oxides with Gd/Fe (molar) = 0.05; 0.10 and 0.15, respectively.

Sample	wt % Fe (±1.0)	wt % Gd (±0.8)	Gd/Fe (molar) (expected)	Gd/Fe (molar) (±0.01) (experimental)
F	68.9	–	–	–
FG05	67.4	9.1	0.05	0.05
FG10	65.4	17.9	0.10	0.10
FG15	63.8	25.4	0.15	0.14
G	–	74.5	–	–

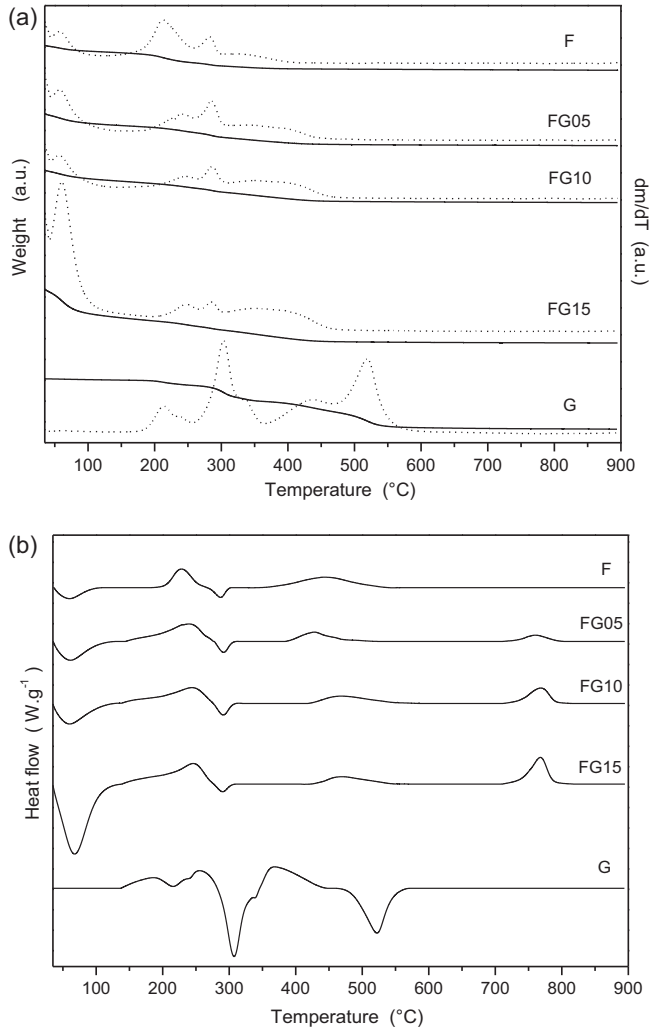

Fig. 1. (a) Thermogravimetry (solid lines) and derivative thermogravimetry (dashed lines) curves and (b) differential scanning calorimetry curves for the catalyst precursors. G: gadolinium oxide; F: iron oxide; FG05, FG10 and FG15: gadolinium and iron oxides with Gd/Fe (molar) = 0.05; 0.10 and 0.15, respectively.

conditions used were appropriate for the precipitation of iron and gadolinium compounds.

The thermogravimetry and derivative thermogravimetry curves of the catalyst precursors (iron and/or gadolinium hydroxide) are shown in Fig. 1a. The gadolinium-free solid (F sample) presented the lowest total weight loss (12.0%) while the FG15 sample showed the highest total weight loss (26.1%). The solids with Gd/Fe = 0.05 and 0.10 showed total weight loss of 15.7 and 15.8%, respectively. For pure iron hydroxide four steps of weight loss were noted. The first one, in the range between 42 and 139 °C is associated with the loss of volatiles including adsorbed water [22]. The second and third peaks, in the range between 185 and 309 °C, are related to partial dehydration of iron hydroxide [22,23]. The weight loss above 300 °C can be attributed to complete dehydration of iron hydroxide to form hematite [22]. It is observed that the presence of gadolinium in solids shifted the second, third and fourth peaks to higher temperatures, indicating that gadolinium made the decomposition of iron hydroxide more difficult, increased by gadolinium content. Pure gadolinium oxide showed weight losses attributed to decomposition of gadolinium of carbonate species occurred simultaneously with dehydration, at temperatures above 400 °C [24]. For all samples no weight loss was observed above 600 °C.

The differential scanning calorimetry curves of the catalyst precursors (Fig. 1b) showed that except for pure gadolinium hydroxide an endothermic peak centered in the range of 55–66 °C can be noted, attributed to the loss of volatiles including water [25], in agreement with the weight loss noted by thermogravimetry in this temperature range. For all curves, an endothermic peak centered in the range of 287–291 °C was found, which is associated to partial dehydration [22]. For gadolinium-containing samples the exothermic peak, characteristic of hematite (centered at around 350 °C for pure iron hydroxide), was shifted to higher temperatures and another exothermic peak centered at 760 °C, attributed to crystallization and the formation of gadolinium ferrite ($FeGdO_3$), was noted [26]. These phase changes were not related to any weight loss as noted by TG curves. These results indicate that gadolinium hinders hematite formation and favors the production of gadolinium ferrite ($FeGdO_3$), instead. The iron-free solid showed endothermic peaks at 220, 440 and 530 °C, assigned to the dehydration process of gadolinium hydroxide ($Gd(OH)_3$) to produce gadolinium oxide (Gd_2O_3) [26] as well as to the decomposition of carbonate species [24]. The curves did not present thermal events at temperatures above 800 °C, indicating the stability of the phases formed.

FTIR spectra for the precursors and for the catalysts are shown in Fig. 2. One can see bands at 3400 and 1630 cm^{-1} attributed to stretching and deformation vibrations of OH water molecules bonds and iron and gadollinium hydroxides [27]. For all spectra, bands in the range of 1380–1600 cm^{-1} can be noted, which are assigned to carbonate groups adsorbed on iron and gadollinum (oxyhydr)oxides [24,28,29]. For all iron-based samples there are absorption bands at 800, 570 and 460 cm^{-1}, which can be related to stretching vibrations of Fe-O bond [30]. FTIR spectrum of iron-free sample showed strong absorptions at 600–400 cm^{-1} related to Gd-O vibration modes [31].

From the X-ray diffractograms for the fresh catalysts (Fig. 3a), it can be noted that the gadolinium-free sample showed a typical pattern of hematite, α-Fe_2O_3, (JCPDS 87-1166) in agreement with previous studies [8,10]. For gadolinium and iron-containing samples, a perovskite phase of gadolinium ferrite, $FeGdO_3$, (JCPDS 78-0451) was also found besides hematite. This finding indicates that the calcination temperature was suitable to the formation of this phase, in accordance with previous work [26]. For the gadolinium-richest sample the cubic phase of gadolinium oxide, Gd_2O_3, (JCPDS 76-0155) was also detected. For the other iron and gadolinium-containing solids, this phase could not be identified because their peaks are coincident with some peaks related to hematite. The iron-free sample showed peaks corresponding to the cubic phase of gadolinium oxide in agreement with previous studies [24], only. After WGSR, the iron-based samples showed different profiles, as shown in Fig. 3b. Magnetite, Fe_3O_4, (JCPDS 19-0629) was found for all iron-based samples, indicating that hematite changed to magnetite during reaction, in agreement with previous works [8,10,12]. For the gadolinium-free sample, iron carbides such as χ-Fe_5C_2 (JCPDS 20-0509) and θ-Fe_5C_2 (JCPDS 76-1877) were also detected. For the iron and gadolinium-containing solids, χ-Fe_5C_2 phase was found while the presence of θ-Fe_5C_2 phase, gadolinium oxide and gadolinium ferrite could not be confirmed because their peaks were coincident among them or with those related to magnetite. Only for the gadolinium-richest sample the presence of gadolinium oxide was confirmed.

The Mössbauer spectra for the fresh catalysts are shown in Fig. 4 and the hyperfine parameters are shown in Table 2. For pure iron oxide, it can be noted a sextuplet whose hyperfine parameters are typical of hematite (α-Fe_2O_3) [32,33]. For the iron and gadolinium-containing samples, the spectra also showed a sextuplet, but the fitting was not suitable with a single interaction, as shown in the internal lateral of the peaks (especially those corresponding to peaks 1 and 6). For this reason, it was

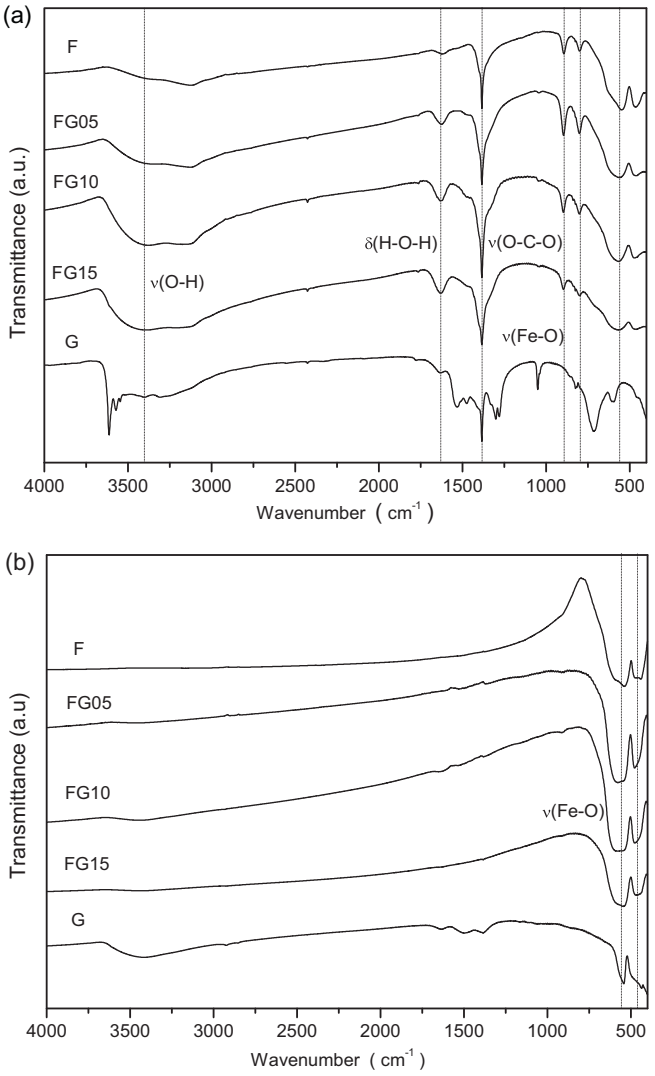

Fig. 2. Fourier transform infrared spectra for (a) the precursors and for (b) the catalysts. G: gadolinium oxide; F: iron oxide; FG05, FG10 and FG15: gadolinium and iron oxides with Gd/Fe (molar) = 0.05; 0.10 and 0.15, respectively.

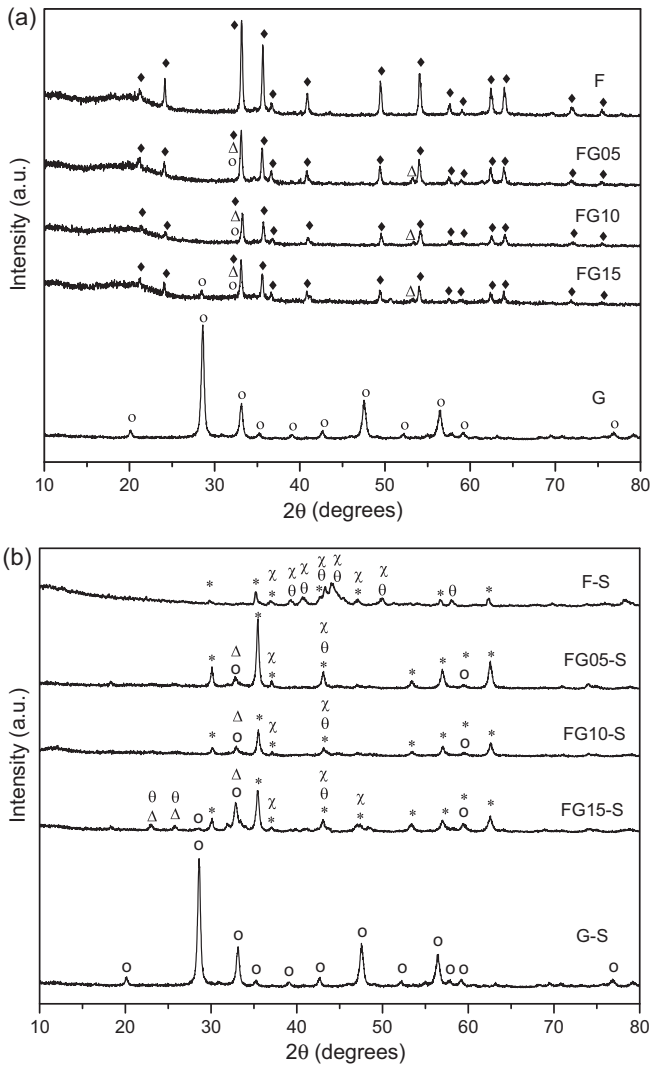

Fig. 3. X-ray diffractograms for the fresh (a) and spent (b) catalysts. G: gadolinium oxide; F: iron oxide; FG05, FG10 and FG15: gadolinium and iron oxides with Gd/Fe (molar) = 0.05; 0.10 and 0.15, respectively. (♦) α-Fe_2O_3; (Δ) $FeGdO_3$; (O) Gd_2O_3; (*) Fe_3O_4; (θ) θ-Fe_3C; (χ) χ-Fe_5C_2.

necessary to include a second sextuplet in the fitting. The sextuplet with the highest hyperfine magnetic field has parameters typical of hematite, similar to gadolinium-free sample. No appreciable decrease for the magnetic hyperfine field as compared to "bulk" hematite was noted. The slight decrease of the magnetic hyperfine field in relation to "bulk" hematite allows the estimative of average crystal sizes for different catalysts using the magnetic collective excitation model [34]. A value of about 150 nm was obtained for all samples.

In order to assign the second sextuplet with lower magnetic hyperfine field, the formation of an iron and gadolinium compound was considered. Among the possible compounds that could be formed in the experimental conditions, $GdFeO_3$ and $Gd_3Fe_5O_{12}$ should be considered [35]. The $GdFeO_3$ compound is a cubic perovskite with all Fe^{3+} ions located in equivalent octahedral sites surrounded by oxygen anions then the Mössbauer spectrum produces a single sextuplet [36,37]. On the other hand, the $Gd_3Fe_5O_{12}$ compound is a gadolinium iron garnet whose general

Table 2
Mössbauer parameters for fresh catalysts at 25 °C. F: iron oxide; FG05, FG10 and FG15: gadolinium and iron oxides with Gd/Fe (molar) = 0.05; 0.10 and 0.15, respectively.

Species	Parameters	F	FG05	FG10	FG15
α-Fe_2O_3	H (T)	51.79 ± 0.01	51.52 ± 0.01	51.56 ± 0.01	51.55 ± 0.01
	δ (mm/s)	0.37 ± 0.01	0.37 ± 0.01	0.37 ± 0.01	0.37 ± 0.01
	2ε (mm/s)	−0.22 ± 0.01	−0.22 ± 0.01	−0.22 ± 0.01	−0.22 ± 0.01
	%	100	94 ± 1	92 ± 1	88 ± 1
$GdFeO_3$	H (T)	–	48.5 ± 0.1	49.5 ± 0.1	49.4 ± 0.1
	δ (mm/s)	–	0.36 (*)	0.40 ± 0.01	0.37 ± 0.01
	2ε (mm/s)	–	0 (*)	0 (*)	0 (*)
	%	–	6 ± 1	8 ± 1	12 ± 1

H: hyperfine magnetic field in Tesla; δ: isomer shift (all the isomer shifts are referred to α-Fe at 25 °C); 2ε: quadrupole shift; △: quadrupole splitting. (*) Parameters held fixed in fitting.

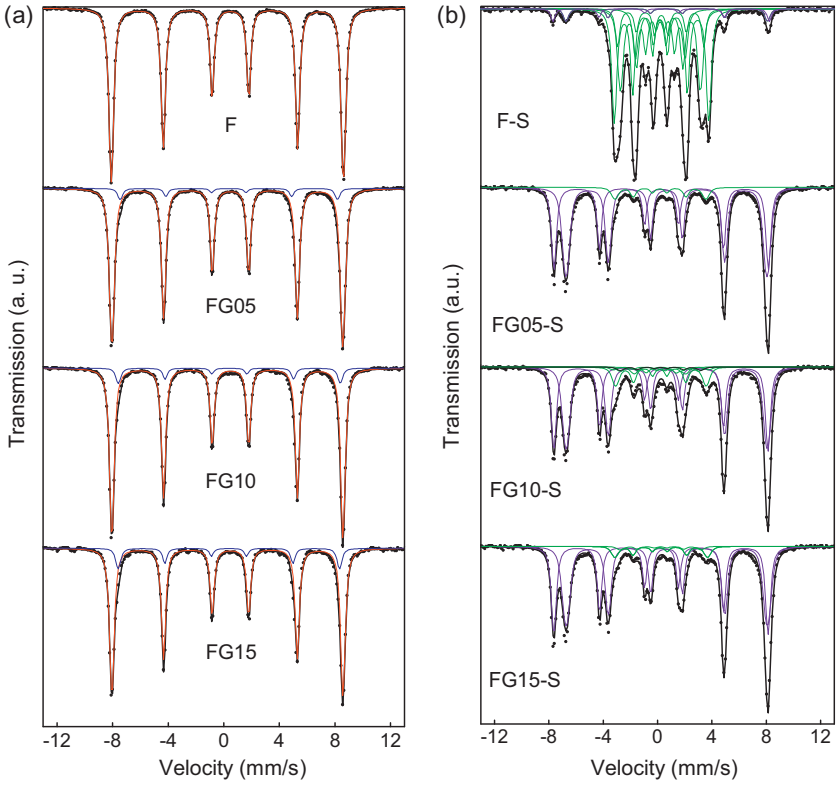

Fig. 4. Mössbauer spectra at 25 °C for the (a) fresh and (b) spent catalysts. G: gadolinium oxide; F: iron oxide; FG05, FG10 and FG15: gadolinium and iron oxides with Gd/Fe (molar) = 0.05; 0.10 and 0.15, respectively. Red line: α-Fe_2O_3; blue line: $GdFeO_3$; green lines: θ-Fe_3C and χ-Fe_5C_2 and purple lines: Fe_3O_4. (For interpretation of the references to color in this figure legend, the reader is referred to the web version of the article.)

formula is $X_3B_2A_3O_{12}$, where Gd^{3+} ions are located in X sites surrounded by eight oxygen anions, whereas Fe^{3+} ions are located in both octahedral (B) and tetrahedral (A) sites with a population ratio of 2:3, respectively. For this reason, the $Gd_3Fe_5O_{12}$ compound produced a Mössbauer spectrum with two clearly distinguishable sextuplets, especially because the signal corresponding to Fe^{3+} ions located at A sites have a magnetic hyperfine field significantly smaller than those at B sites (approximately 40 vs 49 T respectively) [37]. The previous description allows us to rule out the existence of the $Gd_3Fe_5O_{12}$ garnet and confirm the presence of the $GdFeO_3$ perovskite. It is interesting to note that the amount of $GdFeO_3$ phase was lower than that expected taking the Gd/Fe ratio into account. The theoretical weight percentages expected for the FG05, FG10 and FG15 samples would be 14.7, 26.6 and 36.6%, respectively. However, the $GdFeO_3$ percentages detected by Mössbauer spectroscopy were 6 ± 1, 8 ± 1 and $12 + 1$, respectively. Therefore, the excess gadolinium should segregate, probably as gadolinium oxide (Gd_2O_3). This phase was detected by XRD only for the FG15 sample, probably due to the low amount of this phase in the other solids. Therefore, it can be concluded that the catalysts consist of three segregated phases: α-Fe_2O_3, $GdFeO_3$ and Gd_2O_3.

After WGSR, pure iron oxide (F-S sample) showed a very complex Mössbauer spectrum with about nine peaks in the central region (between velocities of about −3.9 and 4.0 mm/s), two peaks in the negative velocities and two other peaks in the positive velocities for iron oxides typical values (Fig. 4b and Table 3). This spectrum was fitted using six sextuplets. Two of them, with the largest magnetic hyperfine fields, can be assigned to Fe^{3+} ions located in A sites and $Fe^{''2.5+''}$ ions located in B magnetite sites (Fe_3O_4) [32,33]. The other four sextets, with low values of magnetic hyperfine fields and isomer shifts, can be assigned to iron carbides, such as cementite (θ-Fe_3C) and to three sites (I, II and III) of Hägg carbide (χ-Fe_5C_2) [38]. The Mössbauer spectra of spent gadolinium-containing catalysts (Fig. 4b and Table 3) changed dramatically as compared to pure iron oxide. All of them showed predominant signals typical of iron ions located in A and B sites of magnetite. In the central region of the spectra only small peaks related to iron carbides were detected. The spectra showed differences depending on gadolinium loading in the solids. For the gadolinium-poorest sample (FG05-S), only an additional sextuplet, assignable to θ-Fe_3C, was necessary to complete the fitting process, probably the three sites of χ-Fe_5C_2 are present in very low concentrations. On the other hand, for FG10-S sample both iron carbides (θ-Fe_3C and χ-Fe_5C_2) with all sites were detected. Finally, for the gadolinium-richest sample (FG15-S) θ-Fe_3C and the I site of χ-Fe_5C_2 were identified. Table 4 displays the amount of iron-containing phase formed in each case. From these results, it can be concluded that the gadolinium-free catalyst is basically made of iron carbides while the iron and gadolinium-based solids are mainly formed by magnetite. Therefore, gadolinium prevents the production of iron carbides. By comparing these results with those obtained by XRD, one can conclude that the iron and gadolinium-containing samples are made of magnetite, iron carbides and gadolinium oxide, since gadolinium ferrite has not been detected by Mössbauer spectroscopy.

The phase changes noted during WGSR can be related to both reducing atmosphere and temperature which are able to produce metallic iron (α-Fe) from hematite (α-Fe_2O_3) during reaction. Fig. 5 illustrated a scheme of the phase changes which is supposed to occur in reaction conditions. Hematite can be transformed to magnetite (Fe_3O_4) and metallic iron (α-Fe) which is able to dissociate carbon monoxide. The carbon atoms can then diffuse inside the α-Fe lattice producing different types of iron carbides. For gadolinium-containing solids, the $GdFeO_3$ perovskite is also reduced but gadolinium (as gadolinium ferrite or as gadolinium oxide) delays iron reduction, as found by TPR. As a consequence,

Table 3
Mössbauer parameters for spent catalysts at 25 °C. F: iron oxide; FG05, FG10 and FG15: gadolinium and iron oxides with Gd/Fe (molar) = 0.05; 0.10 and 0.15, respectively.

Species	Parameters	F	FG05	FG10	FG15
Fe^{3+} in A sites of Fe_3O_4	H (T)	49.4 ± 0.2	48.90 ± 0.02	48.83 ± 0.03	48.86 ± 0.03
	δ (mm/s)	0.28 ± 0.03	0.28 ± 0.01	0.27 ± 0.01	0.27 ± 0.01
	2ε (mm/s)	−0.03 ± 0.05	−0.02 ± 0.01	−0.04 ± 0.01	−0.04 ± 0.01
$Fe^{"2.5+"}$ in B sites of Fe_3O_4	H (T)	46.0 ± 0.2	45.84 ± 0.03	45.86 ± 0.03	45.88 ± 0.04
	δ (mm/s)	0.66 ± 0.03	0.66 ± 0.01	0.66 ± 0.01	0.67 ± 0.01
	2ε (mm/s)	0.03 ± 0.05	0.00 ± 0.01	0.02 ± 0.01	0.02 ± 0.01
θ iron carbide	H (T)	19.7 ± 0.1	20.7 ± 0.2	20.6 ± 0.3	21.1 ± 0.3
	δ (mm/s)	0.25 ± 0.01	0.18 ± 0.02	0.20 ± 0.02	0.22 ± 0.03
	2ε (mm/s)	−0.04 ± 0.02	0.06 ± 0.04	0.09 ± 0.03	0.11 ± 0.05
χ iron carbide site I	H (T)	18.24 ± 0.05	n.d.	17.9 ± 0.7	18.4 (*)
	δ (mm/s)	0.18 ± 0.01	n.d.	0.18 ± 0.06	0.22 (*)
	2ε (mm/s)	0.05 ± 0.01	n.d.	−0.1 ± 0.1	0 (*)
χ iron carbide site II	H (T)	21.55 ± 0.03	n.d.	21.7 (*)	n.d.
	δ (mm/s)	0.24 ± 0.01	n.d.	0.25 (*)	n.d.
	2ε (mm/s)	0.11 ± 0.01	n.d.	−0.01 (*)	n.d.
χ iron carbide site III	H (T)	11.34 ± 0.05	n.d.	11.8 (*)	n.d.
	δ (mm/s)	0.19 ± 0.01	n.d.	0.22 (*)	n.d.
	2ε (mm/s)	0.02 ± 0.01	n.d.	−0.09 (*)	n.d.

H: hyperfine magnetic field in Tesla; δ: isomer shift (referred to α-Fe at 25 °C); 2ε:quadrupole shift; (*) Parameters held fixed in fitting; n.d.: not detected. θ iron carbide: Fe_3C (cementite); χ iron carbide: Fe_5C_2 (Hägg carbide).

Table 4
Amounts of iron phases for spent catalysts obtained from Mössbauer spectra at 25 °C. F: iron oxide; FG05, FG10 and FG15: gadolinium and iron oxides with Gd/Fe (molar) = 0.05; 0.10 and 0.15, respectively.

Sample	% Fe_3O_4	% Iron carbides
F-S	8 ± 1	92 ± 3
FG05-S	93 ± 1	7 ± 1
FG10-S	83 ± 3	17 ± 6
FG15-S	92 ± 1	8 ± 1

Table 5
Specific surface areas of the catalysts before (Sg) and after (Sg*) WGSR performed at 400 °C and hydrogen consumption obtained from TPR curves. G: gadolinium oxide; F: iron oxide; FG05, FG10 and FG15: gadolinium and iron oxides with Gd/Fe = 0.05; 0.10 and 0.15.

Sample	Sg ($m^2\ g^{-1}$)	Sg* ($m^2\ g^{-1}$)	Hydrogen consumption ($\mu mol\ g^{-1}$)
F	10	11	4129
FG05	11	11	2904
FG10	17	17	3831
FG15	12	9	1938
G	18	12	0

only minor quantities of iron carbides are produced and the main phase is magnetite. The production of iron carbides during WGSR does not agree with previous works [8,10]. This can be assigned to the high calcination temperature (800 °C) which seems to favor the production of metallic iron in the conditions of HTS reaction.

The specific surface areas of the solids are presented in Table 5. The values are typically low as a result of the high calcination temperature of the solids. As expected [2,7,26] gadolinium oxide showed a value higher than iron oxide. The addition of gadolinium to iron-based solids generated a solid with higher specific surface areas as compared to pure iron oxide, showing its role as textural promoter. This effect can be assigned to the action of gadolinium as a spacer, creating a barrier among the iron oxide particles and preventing sintering, as noted previously for the ammonia synthesis catalysts [39] and for aluminum-doped iron oxide catalysts for WGSR [8]. Due to the larger Gd^{3+} ions (107 pm) as compared to Fe^{3+} ions (69 pm), they are not expected to enter into hematite or magnetite lattice but rather segregate as gadolinium oxide or as gadolinium ferrite as concluded by Mössbauer spectroscopy and XRD. The sample with the intermediate amount of gadolinium (Gd/Fe = 0.10) showed the highest specific surface area ($17\ m^2\ g^{-1}$) while the gadolinium-poorest sample showed the lowest value. During reaction, the specific surface areas (Table 5) did

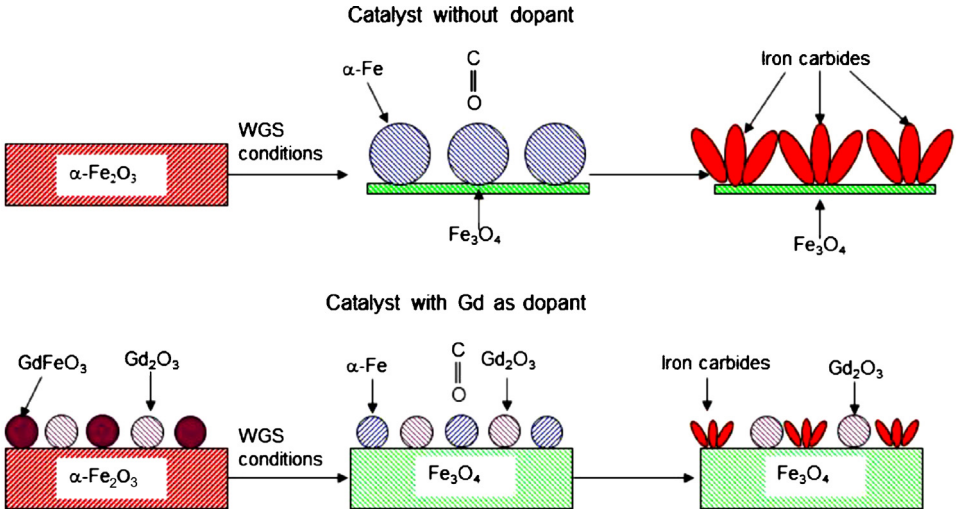

Fig. 5. Scheme showing the phase changes in the catalysts which are expected to occur during WGSR.

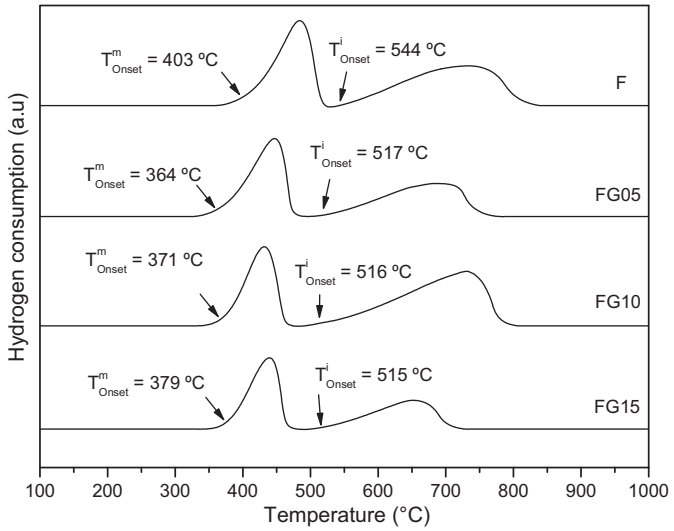

Fig. 6. TPR curves for the catalysts. G: gadolinium oxide; F: iron oxide; FG05, FG10 and FG15: gadolinium and iron oxides with Gd/Fe (molar) = 0.05; 0.10 and 0.15, respectively.

not change significantly, except for the gadolinium-richest sample (FG15), probably due to the presence of larger amount of gadolinium oxide and/or gadolinium ferrite which show typically low specific surface areas.

The curves of temperature programmed reduction for the catalysts are shown in Fig. 6 and the hydrogen consumption during the TPR experiments are shown in Table 5. Pure gadolinium oxide (G sample) showed no reduction peak at the temperature range of the experiment. On the other hand, pure iron oxide (F sample) showed a reduction peak beginning at 403 °C attributed to the reduction of Fe^{3+} to Fe^{2+} species and the peak at higher temperatures beginning at 544 °C related to the reduction of Fe^{2+} to Fe^0 species [8,40]. It can be noted that the gadolinium addition shifted the peaks to lower temperatures. Gadolinium led to a decrease in hydrogen consumption, the reducibility of the solids increased in the order FG15 < FG05 < FG10 < F and then no regular trend could be observed. These findings can be related to different amounts of hematite, gadolinium ferrite and gadolinium oxides as well as to their distribution in the different samples. From these results one can conclude that gadolinium makes the reduction of Fe^{3+} and Fe^{2+} species difficult, probably due to the diffusion effects of hydrogen in the particles of different sizes, as well as to different amounts of these phases in each sample. These results can explain why the gadolinium-containing samples produced less iron carbides from metallic iron.

Fig. 7a shows the conversion of carbon monoxide over the catalysts as a function of reaction temperature. As expected, the conversion increased with temperature due to kinetic factors. At high temperatures (350–400 °C), the catalytic activity of iron oxides increased due to gadolinium and this can be assigned to the ability of this dopant in delaying the production of metallic iron and then iron carbides, as found by TPR and Mössbauer spectroscopy. Therefore, more magnetite is produced in gadolinium-doped samples instead of iron carbides. The activity increased with the dopant amount up to the sample with Gd/Fe = 0.10 (FG10), indicating that there is an optimum amount of gadolinium for its promoter action. As this sample has the smallest amount of magnetite, its superior activity can be related to its highest specific surface area, allowing the exposition of more active sites on the surface. Previous works [5,41] have shown that the HTS reaction occurs over iron-based catalysts through the regenerative mechanism according to which the surface goes on successive cycles of oxidation and

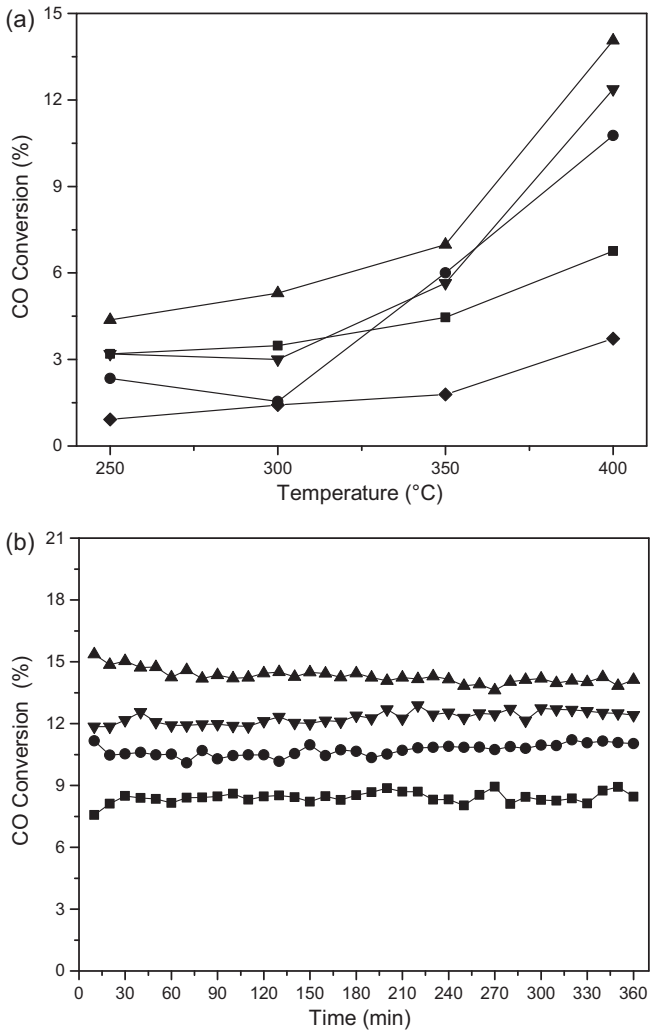

Fig. 7. Conversion of carbon monoxide over the catalysts as a function of (a) reaction temperature and of (b) reaction time in WGSR performed at 400 °C. G (-♦-) sample: gadolinium oxide; (-■-) F sample: iron oxide; (-●-) FG05, (-▲-) FG10 and (-▼-) FG15: gadolinium and iron oxides with Gd/Fe (molar) = 0.05; 0.10 and 0.15, respectively.

reduction by carbon monoxide and water, respectively, to form hydrogen and carbon dioxide. It is well-known that the active phase of hematite-based catalysts is magnetite (Fe_3O_4) [42,43], in which lattice the quantum jumps between the Fe^{2+} and Fe^{3+} levels in the octahedral sites enables the iron oxidation and reduction by water and carbon monoxide, respectively, during WGSR. The low amount of magnetite explains the low activity of free-gadolinium sample [44]. On the other hand, the role of gadolinium ferrite in catalyzing the WGSR has been point out earlier by Haralambous et al. [45,46], who assigned its performance to the presence of point defects in the lattice associated to p-type semi conductivity, favoring the chemisorption of carbon monoxide molecules on their surface [45,46]. However, in the present work gadolinium ferrite is not supposed to play a role, once it is converted to magnetite and iron carbides during reaction.

The results of conversion over catalysts as a function of reaction time, performed at 400 °C for 6 h (Fig. 7b), showed that the catalysts were stable under experimental conditions, indicating that the phase changes occurred in the first minutes of reaction. Only carbon dioxide and hydrogen were detected and no methane or ethane was found for all catalysts, indicating that the iron carbide phases were inactive to Fischer–Tropsch synthesis in the reaction conditions.

4. Conclusions

The hydrolysis of iron nitrate and gadolinium nitrate with ammonia hydroxide, followed by calcination at 800 °C, produces a mixture of hematite, gadolinium oxide (Gd_2O_3) and $GdFeO_3$ perovskite. For these solids, gadolinium leads to an increase of specific surface area and a decrease in reducibility. These catalysts were active in water gas shift reaction (WGSR) and selective only to hydrogen and carbon dioxide. During reaction, they go on phase change, producing magnetite and iron carbides co-existing with gadolinium oxide. The presence of gadolinium inhibits the production of iron carbides, increasing the activity of the catalysts. Iron carbides are inactive to Fischer–Tropsch synthesis and then do not affect the selectivity of the catalysts. The most active catalyst is the solid with Gd/Fe (molar) = 0.1, a fact that was related to its highest specific surface area allowing the exposition of more active sites on the surface.

Acknowledgments

CLSS thanks CNPq for his scholarship. The authors are grateful to Dr. S. T. de Oliva for his help in the X-ray fluorescence analyses. The authors acknowledge CNPq and FINEP for the financial support.

References

[1] D. Holladay, J. Hu, D.L. King, Y. Wang, Catalysis Today 139 (2009) 244–260.
[2] D.S. Newsome, Catalysis Reviews-Science and Engineering 21 (1980) 275–318.
[3] J.L.R. Costa, S.G. Marchetti, M.C. Rangel, Catalysis Today 77 (2002) 205–213.
[4] S.X. Wang, D. Gao, Z. Yuan, N. Liu, C. Zhang, International Journal of Hydrogen Energy 33 (2008) 3710–3718.
[5] L. Lloyd, D.E. Ridler, M.V. Twigg, in: M.V. Twigg (Ed.), Catalysis Handbook, Wolfe Scientific Books, London, 1996, pp. 283–339.
[6] E.M. Fuentes, A.C.F. Júnior, T.F. Silva, J.M. Assaf, M.C. Rangel, Catalysis Today 171 (2011) 290–296.
[7] M.C. Rangel, R.M. Sassaki, F. Galembeck, Catalysis Letters 33 (1995) 237–254.
[8] G.C. Araujo, M.C. Rangel, Catalysis Today 62 (2000) 201–207.
[9] E.B. Quadro, M.L.M. Dias, A.M.M. Amorim, M.C. Rangel, Journal of the Brazilian Chemical Society 10 (1999) 51–59.
[10] A.L.C. Pereira, G.J.P. Berrocal, S.G. Marchetti, A. Albornoz, A.O. de Souza, M.C. Rangel, Journal of Molecular Catalysis A: Chemical 281 (2008) 66–72.
[11] I. Lima Jr., J. Millet, A. Mimoun, M.C. Rangel, Applied Catalysis A-General 283 (2005) 91–98.
[12] A.L.C. Pereira, N.A. dos Santos, M.L.O. Ferreira, L.A.M. Albornoz, M.C. Rangel, Studies in Surface Science and Catalysis 167 (2007) 225–230.
[13] J.Y. Lee, D.W. Lee, K.Y. Lee, Y. Wang, Catalysis Today 146 (2009) 260–264.
[14] C. Martos, J. Dufour, A. Ruiz, International Journal of Hydrogen Energy 34 (2009) 4475–4481.
[15] L. Zhang, J.M.M. Millet, U.S. Ozkana, Journal of Molecular Catalysis A: Chemical 309 (2009) 63–70.
[16] M.S. Santos, G.J.P. Berrocal, J.L.G. Fierro, M.C. Rangel, Studies in Surface Science and Catalysis 167 (2007) 493–498.
[17] P.S. Querino, J.R.C. Bispo, M.C. Rangel, Catalysis Today 108 (2005) 920–925.
[18] J. Tsagaroyannis, K.J. Haralambous, Z. Loizos, G. Petroutsos, N. Spyrellis, Materials Letters 28 (1996) 393–400.
[19] M. Laniecki, M. Ignacik, Catalysis Today 116 (2006) 400–407.
[20] S. Yu Choung, M. Ferrandon, T. Krause, Catalysis Today 99 (2005) 257–262.
[21] C. Wheeler, A. Jhalani, E.J. Klein, S. Tummala, L.D. Schmidt, Journal of Catalysis 223 (2004) 191–199.
[22] A.M. Gadalla, T.W. Levingston, Thermochimica Acta 145 (1989) 1–9.
[23] R. Furuichi, M. Hachiya, T. Ishi, Thermochimica Acta 133 (1988) 101–106.
[24] I.Y. Park, D. Kim, J. Lee, S.H. Lee, K.J. Kim, Materials Chemistry and Physics 106 (2007) 149–157.
[25] R.G. Villacelos, L. Herman, J. Morales, J. Tirado, Journal of Colloid and Interface Science 101 (1984) 393–397.
[26] J. Tsagaroyannis, K.J. Haralambous, Z. Loizos, N. Spyrellis, Materials Letters 14 (1992) 214–221.
[27] R.A. Niquist, R.O. Kagel, Infrared Spectra of Inorganic Compounds, Academic Press, Orlando, 1971.
[28] J.R. Bargar, J.D. Kubicki, R. Reitmeyer, J.A. Davis, Geochimica et Cosmochimica Acta 69 (2005) 1527–1542.
[29] G.A.M. Hussein, Journal of Physical Chemistry 98 (1994) 9657–9664.
[30] S.H. Yariv, E. Mendelovici, Applied Spectroscopy 33 (1979) 410–411.
[31] J.A. Goldsmith, S.D. Ross, Spectrochimica Acta Part A 23 (1967) 1909.
[32] E. Murad, J.H. Johnston, in: G.J. Long (Ed.), Mössbauer Spectroscopy Applied to Inorganic Chemistry, vol. 2, Plenum Publishing Corporation, New York, 1987.
[33] R.E. Vandenberghe, E. De Grave, C. Landuydt, L.H. Bowen, Hyperfine Interactions 53 (1990) 175–196.
[34] S. Mørup, H. Topsøe, Applied Physics 11 (1976) 63–66.
[35] F. Söderlind, L. Selegård, P. Nordblad, K. Uvdal, P.-O. Kall, Journal of Sol-Gel Science and Technology 49 (2009) 253–259.
[36] M. Eibschütz, S. Shtrikman, D. Treves, Physical Review 156 (1965) 562–577.
[37] S.C. Zanatta, L.F. Cotica, A. Paesano, S.N. Medeiros, J.B.M. Cunha, B. Hallouche, Journal of the American Ceramic Society 88 (2005) 3316–3321.
[38] R. L Cohen, Applications of Mossbauer Spectroscopy, vol. II, Academic Press, New York, 1980.
[39] A. Nielsen, H. Bohlbro, Investigation on Promoted Iron Catalysts for the Synthesis of Ammonia, Ed. Gjllerup Forlag, Copenhagen, 1968, pp. p. 221.
[40] J.C. Gonzalez, M.C. Gonzalez, M.A. Laborde, N. Moreno, Applied Catalysis 20 (1986) 3–8.
[41] J.K. Boreskov, T.M. Yureva, A.S. Sergeeva, Kinetics and Catalysis 11 (1970) 1476–1478.
[42] C.H. Bartolomew, R.J. Farrauto (Eds.), Fundamentals of Industrial Catalytic Processes, John Wiley & Sons, Hoboken, NJ, 2006.
[43] C. Lund, Industrial and Engineering Chemistry Research 35 (1996) 2531–2534.
[44] C. Rhodes, G.J. Hutchings, A.M. Ward, Catalysis Today 23 (1995) 43–48.
[45] K.J. Haralambous, Z. Loizos, N. Spyrellis, Materials Letters 11 (1991) 133–138.
[46] K.J. Haralambous, Z. Loizos, N. Spyrellis, Materials Letters 10 (1991) 410–416.